22nd International Conference on Renewable Energies and Power Quality (ICREPQ'24)
Bilbao (Spain), 26th to 28th June 2024

ISBN: 978-84-09-60656-6

The energy balance in a solar-powered UAV flying along the shortest path

A. Ailon

School of Electrical and Computer Engineering
Ben Gurion University of the Negev
Beer Sheva 8410501 Israel
Phone: +97286461518

Abstract. The integration of solar energy into aircraft technology is an attractive and challenging topic, and there is a clear consensus regarding its potential benefits. To optimally apply solar energy, it is important to plan flight paths so that the absorbed energy will be maximal. However, in many missions of Unmanned Aerial Vehicles (UAVs), it is important, sometimes critical to plan the shortest path between two directed points (that is, initial and final positions, each with a defined direction of motion). Therefore, this article deals with combining the issues of planning the shortest route between two directed points and calculating the difference between the collected energy and the consumed energy of a solar-powered UAV when it flies along the shortest path. The article demonstrates how the energy balance depends on the geometry of the shortest path and the position of the sun in the sky, relative to the flying UAV.

Key words. Solar-powered UAV, energy balance, shortest path between endpoints, level flight.

1. Introduction

UAVs are used in a variety of missions, in civil and military applications like surveillance, reconnaissance, and rescue in hostile environments. In such missions flying along the shortest path between two oriented points may be of great importance. Previous studies, for example [1-3], have proposed algorithms for planning the shortest flight path for UAVs by using tools from Dubin's theory [4], which considers the shortest path curve with a constraint on the curvature that connects two points.

The need to increase the endurance and extend the time-of-flight missions motivated researchers [5-12] to study the use solar energy to operate the UAVs in various applications. Since in many situations the flight along a short route is of great practical importance, we are interested in this article to examine the relationship between flight along the shortest path and the resulting energy balance (the difference between the energy provided to the solar system by the sun's radiation and the consumed energy). We recall that the energy balance in a solar-powered UAV depends on both the position of the sun (azimuth and elevation angles with respect to the UAV) [7-8] and the UAV orientation while it follows a reference path. The main current theory in the article is based on the assumption of tracking in open loop of the reference path. However, the article offers a direction for an extension of the research to the case of closed-loop tracking. The article ends with numerical examples.

2. Preliminaries

An approximate aircraft model that flies at a constant height (see Fig. 1) is given by [13]:

$$
\begin{aligned}
\dot{x}(t) &= u(t)cos\psi(t)\\
\dot{y}(t) &= u(t)sin\psi(t)\\
\dot{\psi}(t) &= gL(t)sin\mu(t)/(Wu(t))\\
\dot{u}(t) &= g\left[T(t)-D(t)\right]/W
\end{aligned}
\tag{1}
$$

where T is the thrust, D the drag force, L the lift force, $W=mg$ the UAV's weight (g is the gravitational acceleration), u is the longitudinal velocity with respect to the ground (we assume a still day, no wind, and ground and air velocity, are the same), and ψ,μ are respectively, the heading and the bank angles. Here, the input vector is given by $F(t)=[T(t),\mu(t)]^T$. To ensure that the aircraft does not reach a stalling speed we require that $u(t)\geq\vartheta>0$ where ϑ is a constant. We assume zero pitch, $L=C_L\eta Su^2/2$ and $D=C_D\eta Su^2/2$, C_L and C_D are respectively the lift and drag coefficients, S is the wing planform area, and $\eta=\eta(h)$ is the atmosphere density at height h.

The centripetal force in rotation is $C=mu^2/r$ where r is the instantaneous rotation radius with respect to an instantaneous point of rotation, and m is the aircraft mass. We have $\dot{\psi}=u/r$ and hence $C=mu\dot{\psi}$ or $\dot{\psi}=C/(mu)$. In a constant altitude turn we have $Lcos\mu=mg$, $Lsin\mu=C$ and therefore (see (1)):

$$
\begin{aligned}
\dot{x}(t) &= u(t)cos\psi(t)\\
\dot{y}(t) &= u(t)sin\psi(t)\\
\dot{\psi}(t) &= g(\tan\mu(t))/u(t)\doteq\omega(t)\\
\dot{u}(t) &= g\left[T(t)-D(t)\right]/W.
\end{aligned}
\tag{2}
$$

The solar cells are installed on the upper side of the fixed-wing UAV in Fig. 1 and collect energy from the sun's rays, which we assume (see [7]) is fixed in the sky during the considered process).

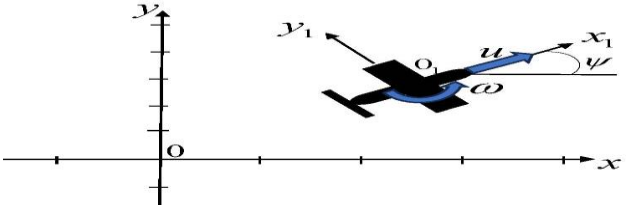

Fig. 1. A schematic model of a solar-powered UAV in level flight with fixed and moving coordinate systems.

Let α, β be respectively the elevation and azimuth of the sun in relation to the UAV. From [7-8] the incidence angle γ of the sun's rays on the solar cells satisfies:

$$cos\gamma(t) = cos\mu(t) sin\alpha - sin\mu(t) cos\alpha sin(\beta - \psi(t)) \quad (3)$$

The power collected by the solar system is given by:

$$P_i(t) = \eta_S P_S S cos\gamma(t) \quad (4)$$

where S is the wings' surface area, η_S is the solar cell efficiency and P_S is the solar spectral density. During the interval $[0, t_f]$ the accumulated energy from the sun is:

$$E_i(t) = \int_0^t \eta_S P_S S cos\gamma(\tau) d\tau,\ t \in [0, t_f] \quad (5)$$

The estimated power lost is:

$$P_o(t) = T(t) u(t) / \eta_p \quad (6)$$

where η_p is the efficiency coefficient of the propeller.

From here the energy loss during the interval $[0, t_f]$ is

$$E_o(t) = \int_0^t T(\tau) u(\tau) / \eta_p d\tau,\ t \in [0, t_f] \quad (7)$$

Then, the difference in the in/out energies during the process is given by:

$$\begin{aligned} E_i(t) - E_o(t) &= \int_0^t (P_i(\tau) - P_o(\tau)) d\tau \\ &= \int_0^t (\eta_S P_S S cos\gamma(\tau) - T(\tau) u_c / \eta_p) d\tau,\ t \in [0, t_f] \end{aligned} \quad (8)$$

3. The energy balance along the shortest path

We assume that the solar-powered UAV flies in a constant altitude and a constant longitudinal speed, namely, $\vartheta \le u(t) = u_c$ and:

$$\dot{u}(t) = g\left[T(t) - D(t)\right] / W = 0 \rightarrow T(t) = D(t) \quad (9)$$

Then (1) reduces to a single input system

$$\begin{aligned} \dot{x}(t) &= u_c cos\psi(t) \\ \dot{y}(t) &= u_c sin\psi(t) \\ \dot{\psi}(t) &= g L(t) sin\mu(t) / (W u_c(t)). \end{aligned} \quad (10)$$

The problem of flying from a point $\{x_0, y_0, \psi_0\}$ to a target $\{x_f, y_f, \psi_f\}$ along the shortest route is associated with the so called Dubin path problem [4], and it typically refers to the shortest curve that connects two points in the two-dimensional space with a constraint on the curvature of the path and with prescribed initial and terminal tangents to the path. Dubin proved that shortest path will be made by joining circular arcs of maximum curvature and straight lines. In more details the shortest path will be at least one of the following six types: RSR, RSL, LSR, LSL, RLR, LRL where 'R' means here a 'right turn', 'L' means a 'left turn', and 'S' means 'flying straight'. For example, if the shortest path is of the type 'RSR', then it corresponds to a right-turn arc 'R' followed by a straight-line segment 'S' followed by a right turn 'R'. Two types of shortest paths from point to point are demonstrated in Figs. 2 and 3.

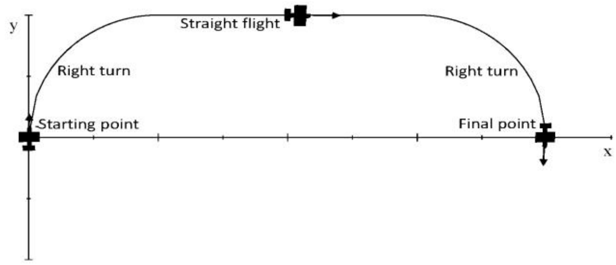

Fig. 2. RSR type shortest path.

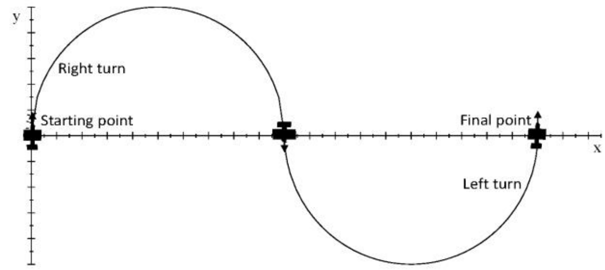

Fig. 3. RSL type shortest path. (In this particular case the segment S shrinks to the contact point of the two circles.)

From previous consideration we can rewrite (1) (recall that $L cos\mu = mg = W$) as

$$\begin{aligned} \dot{x}(t) &= u_c cos\psi(t) \\ \dot{y}(t) &= u_c sin\psi(t) \\ \dot{\psi}(t) &= g(tan\mu) / u_c \end{aligned} \quad (11)$$

We assume that the bank angle is bounded from above and below and let $|\mu| \le \mu_{\max}$. Then the minimum turning radius is given by:

$$\rho = u_c^2 / (g tan\mu_{\max}) \quad (12)$$

We assume that the distance between the centers of the two circular arcs associated with the initial and final points is not smaller than 2ρ.

Next, since we consider a constant speed u_c we have from (8) and the fact that we consider $T = D = C_D \eta S u_c^2 / 2$

$$E_i(t)-E_o(t)=\int_0^t(\eta_S P_S S\cos\gamma(\tau)-T(\tau)u_c/\eta_p)d\tau$$
$$=\int_0^t \eta_S P_S S\cos\gamma(\tau)d\tau-\frac{1}{2}C_D\eta S u_c^3 t/\eta_p,\ t\in[0,t_f] \tag{13}$$

Since Dubins path is defined for a given speed $u_c>0$, the minimum turning radius ρ is given by (12) and the length of the path from a given point to a terminal one can be computed, the arrival time t_f is well defined. For example, in Fig. 2 the path length from point to point appears to be $\pi\rho/2+\pi\rho/2+s=\pi\rho+s$ where s is the distance between the two rotation centers (both are on the x axis) of the two circular parts of the path. Hence, we have $t_f=(\pi\rho+s)/u_c$. Therefore recalling (13) we get:

$$E_i(t_f)-E_o(t_f)=\int_0^{t_f}\eta_S P_S S\cos\gamma(t)dt-\frac{1}{2}C_D\eta S u_c^3 t_f/\eta_p$$
$$=\int_0^{\pi\rho/u_c}\eta_S P_S S\cos\gamma(t)dt+\int_{\pi\rho/u_c}^{s/u_c}\eta_S P_S S\cos\gamma(t)dt \tag{14}$$
$$-\frac{1}{2}C_D\eta S u_c^2(\pi\rho+s)/\eta_p$$

Next, consider the path demonstrated in Fig. 3. In this case the path length from point to point is $2\pi\rho$ and therefore $t_f=2\pi\rho/u_c$. Hence, (13) becomes:

$$E_i(t_f)-E_o(t_f)=\int_0^{t_f}\eta_S P_S S\cos\gamma(t)dt-\frac{1}{2}C_D\eta S u_c^3 t_f/\eta_p$$
$$=\int_0^{2\pi\rho/u_c}\eta_S P_S S\cos\gamma(t)dt-C_D\eta S u_c^2\pi\rho/\eta_p \tag{15}$$

Since in this case we are talking about a pure circular motion of the aircraft (clockwise relative to the center of rotation on the left and then counterclockwise relative to the center of rotation on the left) it can be shown using some elementary trigonometric considerations that for $0\le t<t_f/2=\pi\rho/u_c$ that $\dot\psi(t)=-u_c/\rho$ and for $\pi\rho/u_c\le t\le 2\pi\rho/u_c$, $\dot\psi(t)=u_c/\rho$. Therefore, in the first interval $0\le t<t_f/2=\pi\rho/u_c$ we conclude

$$\psi(t)=\psi(0)+\int_0^t\dot\psi(\tau)d\tau=\pi/2-tu_c/\rho \tag{16}$$

and in the second interval $\pi\rho/u_c\le t\le 2\pi\rho/u_c$

$$\psi(t)=\psi(\pi\rho)+\int_{\pi\rho/u_c}^t\dot\psi(\tau)d\tau=-3\pi/2+tu_c/\rho \tag{17}$$

Therefore, by referring to (13) the computation of the energy balance at the end of the process gives:

$$E_i(t_f)-E_o(t_f)=\int_0^{t_f}\eta_S P_S S\cos\gamma(t)dt-\frac{1}{2}C_D\eta S u_c^3 t_f/\eta_p$$
$$=\int_0^{\pi\rho/u_c}\eta_S P_S S\cos\gamma(t)dt+\int_{\pi\rho/u_c}^{2\pi\rho/u_c}\eta_S P_S S\cos\gamma(t)dt \tag{18}$$
$$-C_D\eta S u_c^2\pi\rho/\eta_p$$

Using (3) we have in the present case (note that $\mu=\mu_{\max}$ in the time period $0\le t<\pi\rho/u_c$ and $\mu=-\mu_{\max}$ in $\pi\rho/u_c\le t<2\pi\rho/u_c$):

$$\cos\gamma(t)=\cos\mu_{\max}\sin\alpha-\sin\mu_{\max}\cos\alpha\sin(\beta-\psi(t))=$$
$$\cos\mu_{\max}\sin\alpha-\sin\mu_{\max}\cos\alpha(\cos\psi(t)\sin\beta-\sin\psi(t)\cos\beta) \tag{19}$$

and respectively in $\pi\rho/u_c\le t<2\pi\rho/u_c$

$$\cos\gamma(t)=\cos\mu_{\max}\sin\alpha+\sin\mu_{\max}\cos\alpha\sin(\beta-\psi(t))=$$
$$\cos\mu_{\max}\sin\alpha+\sin\mu_{\max}\cos\alpha(\cos\psi(t)\sin\beta-\sin\psi(t)\cos\beta) \tag{20}$$

Recalling that $\mu_{\max},\alpha,\beta$ are constants and $\psi(t)$ is linear in t in both intervals (see (16)-(17)) the energy balance in (18) can finally be computed.

4. Practical tracking of the shortest path

In the previous section we assumed that the solar-powered UAV follows exactly the desired shortest path. But from a practical point of view, one needs to implement a controller that will ensure that in the practical sense tracking indeed holds. For this, we need to implement a trajectory following control lawstrategy. To this end we assume in the coming discussion that the longitudinal positive speed $u(t)$ and the bank angle $\mu(t)$ are regarded as input signals and if a small error occurs during the flight between the actual path and the desired Dubins path, $u(t)$ is almost constant and $T\approx D$. We confine the discussion to the case when Dubins path can be represented by a function $y=f(x)$ in a given interval $[x_0,x_f]$ where $x_0=x(0),x_f=x(t_f)$. Note that in the current case we consider a piecewise-defined function in the (x_0,x_f) interval and present it as:

$$y=f(x)=\begin{cases}c_1(x),x_0\le x<x_1\\ s(x),x_1\le x<x_2\\ c_2(x),x_2\le x<x_f\end{cases} \tag{21}$$

where $c_i(x),i=1,2$ refer to the 'right/left turn' segments and $s(x)$ refers to the straight flight segment. We emphasize that $f(x)$ and $\partial f(x)/\partial x$ are continuous in (x_0,x_f). This is so because the line associated with straight flight is tangent to both curves. Let (11) be replaced by (the model that represents the real UAV)

$$\dot{x}(t)= u(t)cos\psi(t)$$
$$\dot{y}(t)= u(t)sin\psi(t) \quad (22)$$
$$\dot{\psi}(t)=\omega(t)$$

where $\omega(t) \doteq g \tan \mu(t) / u(t)$. Suppose that the Dubins path satisfies the equation (the model of the virtual UAV, namely, UAV*)

$$\dot{x}^*(t)= u_c cos\psi^*(t)$$
$$\dot{y}^*(t)= u_c sin\psi^*(t) \quad (23)$$
$$\dot{\psi}^*(t)=\omega^*(t)$$

where $\omega^*(t) \doteq g(\tan \mu^*(t)) / u_c$, $\mu^*(t)$ is the input, and u_c is constant with $u_c = \sqrt{\left(\dot{x}^*(t)\right)^2 + \left(\dot{y}^*(t)\right)^2}$.

Regarding the UAV* we have

$$\dot{x}^*(t) = u_c / \sqrt{1+(\partial f(x^*)/\partial x^*)^2}$$
$$\dot{y}^*(t) = (\partial f(x^*) / \partial x^*) u_c / \sqrt{1+(\partial f(x^*)/\partial x^*)^2} \quad (24)$$

where the variables marked with a star satisfy the equation $y^*(t) = f(x^*(t))$ associated with the UAV* that flies along Dubins path. Note: $(\partial f(x^*) / \partial x^*)$ depends on t.

Let $\varphi = [x, y, \psi]^T, \varphi^* = [x^*, y^*, \psi^*]^T$ be respectively the trajectories of (22) and (23). Roughly, the purpose of the controller is to ensure that the trajectory φ will be "close" to φ^* during the time interval $t \in [0, t_f]$. Let $e = [e_1, e_2, e_3]^T \doteq [x - x^*, y - y^*, \psi - \gamma]^T$ be the error vector, where γ will be defined shortly. We need to distinguish between the following two cases: (i)- $\dot{x}^*(t) \geq \delta > 0, \forall t \in [0, t_f]$, (ii)- $\dot{x}^*(t) \geq 0, \forall t \in [0, t_f]$ where δ is a selected constant. Since Dubins path is a-priori known, $\dot{x}^*(t)$ & $\dot{y}^*(t)$ are given by (24). In Figs. 2 & 3 the situations correspond to case (ii). With reference to case (ii) we will only make a general comment here

Recall the condition in case (i) and letting

$$\lambda_x \doteq \dot{x}^* - atanh(ke_1),\ \lambda_y \doteq \dot{y}^* - btanh(le_2) \quad (25)$$

where $a,b,k,l > 0$ are constants and $a < \delta$. Then $\lambda_x(t) \geq \xi > 0, \forall t \in [0, t_f]$ where ξ is a constant. Let

$$\gamma \doteq \arctan(\lambda_y / \lambda_x),\ u \doteq \sqrt{\lambda^2{}_x + \lambda^2{}_y},\ \omega \doteq \dot{\gamma} - \alpha e_3 \quad (26)$$

where $\alpha > 0$ is a constant. (By definition $u > 0$ is bounded from above and below.) Then we have

$$ucos\gamma = \lambda_x,\ usin\gamma = \lambda_y. \quad (27)$$

We can rewrite (22) as

$$\dot{x}= ucos\psi + ucos\gamma - ucos\gamma$$
$$\dot{y}= usin\psi + usin\gamma - usin\gamma \quad (28)$$
$$\dot{\psi}=\dot{\gamma}-\alpha e_3$$

Then, using (26)-(27) the error dynamics is given by

$$\dot{e}_1= -atanh(ke_1)+u(cos\psi - cos\gamma)$$
$$\dot{e}_2= -btanh(ke_2)+u(sin\psi - sin\gamma) \quad (29)$$
$$\dot{e}_3= -\alpha e_3$$

Applying some trigonometry identities, we have $|cos\psi - cos\gamma| = |2\sin((\psi-\gamma)/2)\sin((\psi+\gamma)/2)| \leq |e_1|$ and similarly $|\sin\psi - \sin\gamma| \leq |e_2|$. Therefore, since $u(t)$ in (26) is bounded and we can prove using the arguments of [14] that the trivial solution of (29) is globally asymptotically stable and thus the suggested controller will keep $\varphi(t)$ "close" to $\varphi^*(t)$.

In case (ii) the situation is a bit more complicated since we can't use the fact that $\lambda_x(t)$ is larger than zero for all $t \in [0, t_f]$ and thus γ in (26) is not well defined. To apply the design approach for case (ii), it is possible to apply a coordinate transformation (using a 2×2 rotation matrix), which will allow avoiding singularities in the case of $\lambda_x(t_i) = 0$ at the relevant points $t_i \in [0, t_f]$.

5. Examples

We use the MKS system of units: meter-kilogram-second. Let $u_c = 24m./\sec.$, $\vartheta = 15m./\sec.$, and $\mu_{\max} = \pi/4rad.$ (recall that $u_{\min} \geq \vartheta$ and $|\mu| \leq \mu_{\max}$). The wing area is $S = 10m.^2$. The atmosphere density is $\eta = 1.1kg./m.^3$ and the propeller efficiency is η_p=0.9. The solar cell efficiency is $\eta_S = 0.75$ and the solar spectral density is $P_S = 1200w./m.^2$. The drag coefficient is $C_D = 0.1$. Let the initial state of the system (10) be $\varphi_0 = [x_0, y_0, \psi_0]^T = [0, 0, -\pi/4]^T$ where $\varphi_0 \doteq \varphi(0)$. The control objective is to fly to the target $\varphi_f = [x_f, y_f, \psi_f]^T = [1000, 0, -\pi/3]^T$, $\varphi_f \doteq \varphi(t_f)$ along the shortest path & to calculate the energy balance.

Example 1. Suppose that the elevation and azimuth angles are given respectively by $\alpha = \pi/2rad.$, $\beta = \pi/4rad.$.

A. Determining the shortest path

By using basic trigonometric tools, it is possible to determine useful relevant points. The centers are located on the lines perpendicular to the flight directions at the starting and ending points and at a distance ρ (see (12)), which is the circles' radius. The coordinates of the center of the circle associated with the initial point are

$$x_{ci} = x(0) + \rho cos(\pi/2 - \psi(0)) = \rho cos(\pi/4) = 0.707\rho$$
$$y_{ci} = y(0) + \rho sin(\pi/2 - \psi(0)) = \rho sin(\pi/4) = 0.707\rho \quad (30)$$

As for the second circle, the center's coordinates are:

$$x_{cf} = x(t_f) - \rho cos(\pi/2 - \psi(t_f)) = 1000 - 0.866\rho$$
$$y_{cf} = y(t_f) - \rho sin(\pi/2 - \psi(t_f)) = -0.5\rho \tag{31}$$

The distance s between the circles' centers is given by:

$$s = \sqrt{(x_{cf} - x_{ci})^2 + (y_{cf} - y_{ci})^2} \tag{32}$$

The coordinates of the transition point from the left circular flight to the flight along a straight line are:

$$x_{di} = x_{ci} + \rho sin(\pi/2 - arccos(\rho/(s/2)))$$
$$y_{di} = y_{ci} - \rho cos(\pi/2 - arccos(\rho/(s/2))) \tag{33}$$

The coordinates of the transition point from the flight along a straight line to the right circular flight are:

$$x_{df} = x_{cf} - \rho sin(\pi/2 - arccos(\rho/(s/2)))$$
$$y_{df} = y_{cf} + \rho cos(\pi/2 - arccos(\rho/(s/2))) \tag{34}$$

In the considered case the numerical values are (see (12), and (29)-(33))

$$\rho = u_c^2/(gtan\mu_{\max}) = 576/9.8 = 58.78, s = 910.30$$
$$\{x_{ci}, y_{ci}\} = \{41.57, 41.57\}; \{x_{cf}, y_{cf}\} = \{949.10, -29.39\} \tag{35}$$
$$\{x_{di}, y_{di}\} = \{49.16, -16.72\}; \{x_{df}, y_{df}\} = \{941.51, 28.90\}$$

Fig. 4 shows the shortest flight path between the points $\varphi_0 = [0, 0, -\pi/4]^T$ and $\varphi_f = [1000, 0, -\pi/3]^T$.

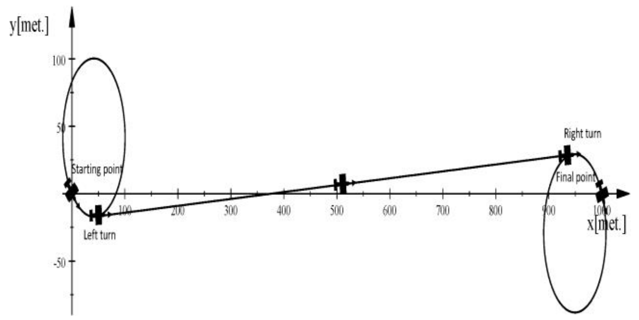

Fig. 4. The LSR type Dubin path between the states φ_0 and φ_f.

Comment: the left and right turning segments are slightly distorted in the figure due to the different scale of the axes x, y.

B. The heading angle along the shortest path

We first need to define the time intervals associated with each segment, as well as the final time t_f. For this we first compute the path segments length. In the left turn section, the length s_l is given by (see (33)-(35)):

$$s_l = \rho 2arcsin\left(\frac{\sqrt{(x_{di} - x_0)^2 + (y_{di} - y_0)^2}}{2\rho}\right) = 53.78$$

The length s_s of the straight segment is:

$$s_s = \sqrt{(x_{df} - x_{di})^2 + (y_{df} - y_{di})^2} = 893.52\,.$$

In the right turn section of the path, the length s_r is computed as follows:

$$s_r = \rho 2arcsin\left(\frac{\sqrt{(x_f - x_{df})^2 + (y_f - y_{df})^2}}{2\rho}\right) = 69.16$$

Hence, the total length s_t of the shortest path is given by:

$$s_t = 53.78 + 893.52 + 69.16 = 1016.50 \tag{36}$$

Recalling that $u_c = 24$, from (36) the time durations to complete the left turn t_{fl}, the straight line flight t_{fs}, the right turn flight t_{fr}, and the final time t_f are respectively:

$$t_{fl} = 53.78/24 = 2.24; t_{fs} = 893.52/24 = 37.23$$
$$t_{fr} = 69.16/24 = 2.88; t_f = 1016.50/24 = 42.35 \tag{37}$$

Next, we need to determine the time function $\psi(t)$ along the path. During the left turning, the straight flight, and the right turning we have respectively:

$$\psi(t) = \psi_0 + \int_0^t u_c/\rho d\tau = -\pi/4 + 0.41t,\ t \in [0, t_{fl}]$$
$$\psi \doteq \psi_c = -\pi/4 + 0.41 * 2.24 = 0.13,\ t \in (t_{fl}, t_{fl} + t_{fs}]$$
$$\psi(t) = \psi_c - \int_{t_{fl}+t_{fs}}^{t} u_c/\rho d\tau = 0.13 - 0.41(t - (t_{fl} + t_{fs}),$$
$$t \in (t_{fl} + t_{fs}, t_f] \tag{38}$$

The UAV heading as a function of time is given in Fig. 5.

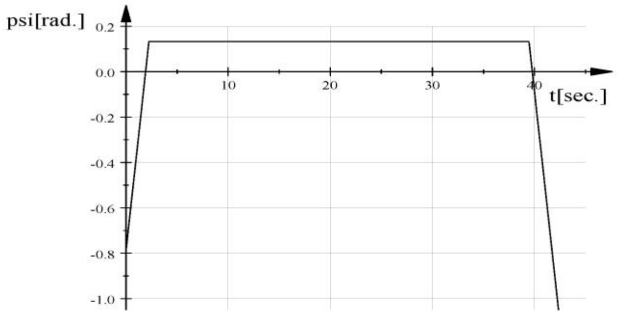

Fig. 5. Time history of the heading angle along the shortest path.

C. The energy balance along the shortest path

To compute the energy balance, we apply equations (3) and (13). Since $\alpha = \pi/2, \beta = \pi/4$ and along the circle segments $|\dot{\psi}(t)| = u_c/\rho$ while along the straight-line $\dot{\psi}(t) = 0$, equation (3) becomes:

$$cos\gamma(t) = cos\mu(t) = \begin{cases} cos(\pi/4), & t \in [0, t_{fl}] \\ cos(0), & t \in (t_{fl}, t_{fl} + t_{fs}] \\ cos(-\pi/4), & t \in (t_{fl} + t_{fs}, t_f] \end{cases} \tag{39}$$

From (13) we have:

$$E_i(t) - E_o(t) = \int_0^t (\eta_S P_S S cos\gamma(\tau) - \frac{1}{2} C_D \eta S u_c^{\,3} / \eta_p) d\tau \quad (40)$$

Integrating the piecewise function and recalling (38)-(39):

$$E_i(t) - E_o(t) = \begin{cases} -2085t, \ 0 \le t \le 2.24 \\ -5907 + 552t, \ 2.24 < t \le 39.47 \\ 98175 - 2085t, \ 39.47 < t \le 42.35 \end{cases} \quad (41)$$

The results are plotted in Fig. 6 below.

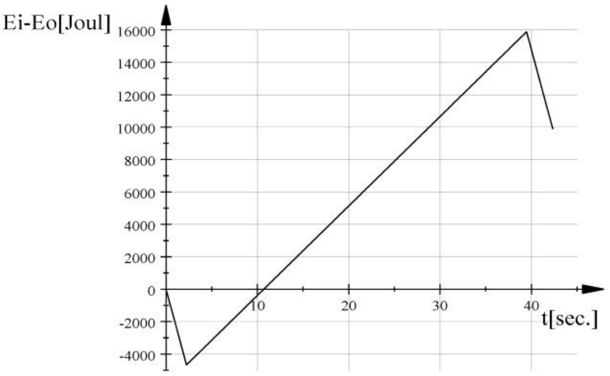

Fig. 6. The energy balance along the three path segments (Ex. 1).

Example 2. Let the altitude and azimuth angles be $\alpha = \pi/3, \ \beta = \pi/6$ and the rest of the data is the same as in Example 1. Then, the shortest path is the same as in the previous example and (see (3)):

$$cos\gamma(t) = 0.87 cos\mu(t) - 0.5 sin\mu(t) sin(\pi/6 - \psi(t)) \quad (42)$$

To compute the energy balance along the shortest path we use (40)-(41) where $cos\gamma(t)$ is given by the right-hand side of (42) with $\psi(t)$ in (38), $cos\mu(t)$ by the right-hand side of (39) and similarly by replacing $cos\mu(t)$ with $sin\mu(t)$ in (39). Then, the energy balance is given by

$$E_i(t) - E_o(t) = \begin{cases} -2008 cos(0.41t) - 7495 sin(0.41t) \\ \quad - 2912t - 2008 \ , \ 0 \le t \le 2.24 \\ \quad - 618t - 27.92, \ 2.24 < t \le 39.47 \\ (sin(0.41t - 15.8))(3181.5t - 1.256 * 10^5) \\ \quad - 2912.2t + 90579, \ 39.47 < t \le 42.35 \end{cases} \quad (43)$$

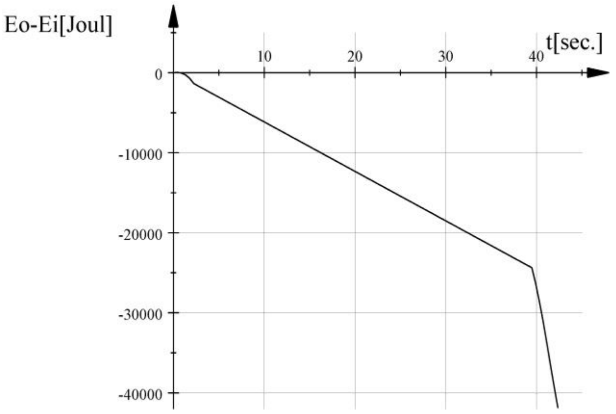

Fig. 7. The energy balance along the three path segments (Ex. 2).

6. Conclusion

In this study we investigate two issues related to the flight planning of a solar-powered UAV. We are mainly interested in the question of what the energy consumption is compared to the energy absorbed from the sun in the UAV's solar system when flying along the shortest route from origin to final destination. (It should be indicated that the flight from an initial state to a final one at a constant speed along the shortest route means arriving at the goal in minimum time.) In particular we demonstrated how a change in the energy balance, which depends on the position of the sun, the azimuth and elevation angles with respect to the UAV that follows the shortest path. Also, it is naturally appealing to expand the part where the control strategy allows the presentation of a control design for a more practical application, especially with an emphasis on the design of a closed loop control system for tracking the desired flight path. A possible approach in this direction was presented in this article, but further research is still required and is actually underway.

References

[1] I. Lugo-Cardenas, G. Flores, S. Salazar, & R. Lozano, "Dubins path generation for a fixed wing UAV," *Inter. Conf. on Unmanned Aircraft Systems (ICUAS)*, Orlando, May 2014.

[2] H. Chitsaz & S. M. LaValle, "Time-optimal paths for a Dubins airplane," *Proc. of the 46th IEEE Conf. on Decision and Control (CDC)*, New Orleans, Dec. 2007.

[3] P. Yan, Z. Yan, H. Zheng, and J, Guo, "A fixed wing UAV path planning algorithm based on genetic algorithm and Dubins curve theory," MATEC Web of Conferences 179, 03003, pp.1-10 https://doi.org/10.1051/matecconf/201817903003, 2018.

[4] L. E. Dubins, "On curves of minimal length with a constraint on average curvature, and with prescribed initial and terminal positions and tangents," *American Journal of Mathematics*, vol. 79, pp. 497–516, 1957.

[5] P. Oettershagen, A. Melzer, T. Mantel, K. Rudin; T. Stastny; B. Wawrzacz; T. Hinzman, K. Alexis, and R. Siegwart, "Perpetual flight with a small solar-powered UAV: Flight results, performance analysis and model validation," *IEEE Aerospace Conference*, Big Sky, MT, USA, 2016.

[6] W. Ni, W. Di, & X. Ma, "Energy-optimal flight strategy for solar-powered aircraft using reinforcement learning with discrete actions" IEEE Access, Vol. 4, pp. 1-22, 2016.

[7] A.T. Klesh & P.T. Kabamba, "Energy-Optimal path planning for solar-powered aircraft in level flight," *Proc. AIAA Guide., Nav. & Contr. Conf.*, S. Carolina, USA, Aug. 2007.

[8] A. T. Klesh & P. T. Kabamba, "Solar-powered aircraft: energy-optimal path planning and perpetual endurance," *J. Guide. Contr., Dyn*. Vol. 32, pp. 1320-1329, 2009.

[9] H. Huang & A.V. Savkin, "Autonomous navigation of a solar-powered UAV for secure communication in urban environments with eavesdropping avoidance," *Future Internet*, Vol. 12, pp. 1-22, https://doi.org/10.3390/fi12100170, 2020.

[10] A. Ailon, "A path planning approach for unmanned solar-powered aerial vehicles," *Renewable Energies and Power Quality Journal*, vol. 21, pp. 109-114, 2023.

[11] K. Mateja, W. Skarka, M. Peciak, R. Niestrój & M. Gude, "Energy autonomy simulation model of solar powered UAV," *Energies*, Vol. 16, pp. 1-31, https://doi.org/10.3390/en16010479, 2023.

[12] S. Morton, R. D'Sa, and N. Papanikolopoulos, "Solar powered UAV: design and experiments," *IEEE/RSJ International Conference on Intelligent Robots and Systems (IROS)*, Hamburg, Germany, 2015.

[13] D. G. Hull, Fundamentals of Airplane Flight Mechanics, Springer-Verlag, Berlin Heidelberg 2007.

[14] A. Ailon, "Trajectory tracking for UAVs with bounded inputs and some associated applications," *Proc. 6th IFAC Symp. Rob. Contr. Design (ROCOND)*, Haifa, Israel, Jun. 2009.